Antibacterial and Cell-adhesive Polypeptide and Poly(ethylene glycol) Hydrogel as a Potential Scaffold for Wound Healing

Airong Song[a], **Aboli A. Rane**[a], and **Karen L. Christman**[a,*]

[a]Bioengineering Department, University of California, San Diego, CA, 92093

Abstract

The ideal wound healing scaffold should provide the appropriate physical and mechanical properties to prevent secondary infection, as well as an excellent physiological environment to facilitate cell adhesion, proliferation and/or differentiation. Therefore, we developed a synthetic cell-adhesive polypeptide hydrogel with inherent antibacterial activity. A series of polypeptides, $poly(Lys)_x(Ala)_y$ (x+y=100) with varied hydrophobicity via metal-free ring-opening polymerization of NCA-Lys(Boc) and NCA-Ala monomers (NCA = N-carboxylic anhydride) mediated by hexamethyldisilazane (HMDS) were synthesized. These polypeptides were cross-linked with 6-arm PEG-amide succinimidyl glutarate (ASG) (M_w = 10K) to form hydrogels with a gelation time of five minutes and a storage modulus (G') of 1400–3000 Pa as characterized by rheometry. The hydrogel formed by cross-linking of $poly(Lys)_{60}(Ala)_{40}$ (5 wt%) and 6-arm PEG-ASG (16 wt%) (Gel-III) exhibited cell adhesion and cell proliferation activities superior to other polypeptide hydrogels. In addition, Gel-III displays significant antibacterial activity against *E. coli* JM109 and *S. aureus* ATCC25923. Thus, we have developed a novel, cell-adhesive hydrogel with inherent antibacterial activity as a potential scaffold for cutaneous wound healing.

Keywords

Hydrogel; Antibacterial; Cell-adhesive; Wound healing; Polypeptide

1. Introduction

Wound healing typically occurs through the process of hemostasis, inflammation, tissue repair and remodeling [1–2]. However, some wounds, such as diabetic ulcers, burns, or arterial ulcers, develop into chronic wounds that do not heal [3]. Conventional wound dressings are composed of fabric materials that protect the wound site from external contamination [4–5]; however, they do not provide an appropriate environment for tissue repair and regeneration. Advanced dressings, including both biological and synthetic scaffolds, can provide a physical barrier against secondary infection, as well as a compatible physiological environment [4–6]. Biological dressings, such as allografts [7–8], xenografts [9–10], reconstituted collagen-based matrices [5, 11–12], hyaluronan-based scaffolds [13–15], and chitosan-based scaffolds [16–18], can greatly improve quality of healing, and

*Corresponding author at: Department of Bioengineering, University of California, San Diego, USA. Tel.: +1 858 822 7863; Fax: +1 858 534 5722. christman@bioeng.ucsd.edu.

Publisher's Disclaimer: This is a PDF file of an unedited manuscript that has been accepted for publication. As a service to our customers we are providing this early version of the manuscript. The manuscript will undergo copyediting, typesetting, and review of the resulting proof before it is published in its final citable form. Please note that during the production process errors may be discovered which could affect the content, and all legal disclaimers that apply to the journal pertain.

decrease healing time [5]. However, concerns with biological scaffolds are their poor biostability, low mechanical properties, high cost, low shelf-life, risks of immunological rejection, and lot-to-lot variability [6]. Synthetic dressings have been developed to overcome these problems [6]. Many synthetic polymers, including polyurethane (PU) [19], polyglycolic acid/polylactic acid (PLGA) [20], poly(L-lactide) (PLLA) [21], polycaprolactone (PCL) [22], peptide nanofibers [23] and poly(ethyleneglycolterephthalate)-poly (butyleneterephthalate) copolymer et al. [21], have been examined with or without natural polymers for wound repair and tissue regeneration.

An ideal wound healing scaffold should include these characteristics: appropriate physical and mechanical properties to prevent secondary infection, and excellent physiological environment to facilitate cell adhesion, proliferation and/or differentiation. Among synthetic dressings, hydrogels with inherent antibacterial activity are particularly advantageous since they can prevent water loss and secondary infection when exposed to the environment, absorb wound fluids, and provide adequate gaseous exchange [24–28]. These materials can improve cell adhesion and proliferation, and prevent infection, while no harsh sterilization is required [28]. Antimicrobial hydrogels have been prepared through encapsulation of antibacterial molecules into the hydrogel scaffold [25, 29–32], or self-assembly of alternating Lys-Val peptides [28]. However, limitations with the above two approaches are the fast release of antibiotics with the former, and the high cost, difficult preparation and poor tunability in terms of incorporating of other bioactive agents with the latter.

To overcome these limitations, we prepared an easily synthesized cell-adhesive hydrogel with inherent antibacterial activity based on chemical cross-linking between a polypeptide and 6-arm polyethylene glycol (PEG)-amide succinimidyl glutarate (ASG). The presence of lysine or arginine in antimicrobial peptides (AMPs) and their amphiphilic structures are known to inhibit bacterial growth [33]. Thus, lysine was used in the generated polypeptides not only as a cross-linker for 6-arm PEG-ASG but also for its anti-microbial properties. To make antibacterial hydrogels, we synthesized a series of biodegradable polypeptides poly(Lys)$_x$(Ala)$_y$ (x+y=100) with varied cationic/hydrophobic balance via ring-opening polymerization (ROP) of NCA-Lys(Boc) 1 and NCA-Ala 2 monomers (NCA = N-carboxylic anhydride) mediated by hexamethyldisilazane (HMDS) [34]. The amphipathic conformation of AMPs can facilitate binding to and insertion into bacterial membranes [33]. The subsequent membrane disruption [33], membrane depolarization [35], or inhibition of cell wall synthesis [36] is thought to lead to bacterial cell death. We demonstrate that only the poly(Lys)$_{60}$(Ala)$_{40}$ (Polypeptide-3) and 6-arm PEG-ASG cross-linked hydrogel Gel-III displayed both antibacterial and cell adhesive properties. This new hydrogel, therefore, has the potential to be a new tissue engineering scaffold for wound healing.

2. Matereials and Methods

2.1 Materials and general methods

6-arm PEG-ASG (M.W. = 10K) was purchased from Sunbio PEG-shop. H-Lys(Boc)-OH was purchased from Aroz Technologies (Cat # HK-0201). Trilysine and L-Alanine were obtained from Sigma-Aldrich (Milwaukee, WI) (Cat # L8901 and 05130). Triphosgene was purchased from TCI America (Cat # T1467). All the dry solvents were used as received and handled under dry argon. Collagen Type I (rat tail) concentrated solution was bought from BD Biosciences (Cat # 354249). All reactions were carried out under an Ar atmosphere in oven-dried glassware unless otherwise specified. Inova300 and Inova400 MHz NMR Instruments were used to perform NMR analysis, and spectra were recorded in CDCl$_3$ or CD$_2$Cl$_2$ unless otherwise noted. ^{1}H-NMR spectra are reported as chemical shift in parts per million (multiplicity, coupling constant in Hz, integration). ^{1}H-NMR data are assumed to be first order. All NMR spectra are shown in the supporting information. LIVE/DEAD

viability/cytotoxicity kit for mammalian cells (L3224), LIVE/DEAD BacLight bacterial viability kit (L13152), Quant-iT PicoGreen dsDNA reagent and kit (P7589) and Vybrant MTT cell proliferation assay kit (V13154) were purchased from Invitrogen. *E. coli* strain (JM109) was purchased from Agilent Technologies, and *S. aureus* strain (ATCC 25923) was purchased from VWR International. Light scattering (OD625nm) was measured on a UV-Visible Spectrophotometer employing a 1 cm pathlength cell. NIH3T3 fibroblasts were cultured in 90% Dulbecco's Modified Eagle's Medium (DMEM) with PenStrep glutamine (50 units/mL penicillin, 50 μg/mL streptomycin, 146 μg/mL L-glutamine), and 10% bovine calf serum.

2.2 Monomer synthesis

NCA monomers, NCA-Lys(Boc) 1 and NCA-Ala 2 were synthesized via reaction of their corresponding amino acids with triphosgene (Fig. S1) [37]. As a high purity of NCA monomers are required for anionic ROP reactions [38], the NCA monomers were recrystallized three times from THF/hexane to provide ultra pure products for ROP.

NCA-Lys(Boc), 1. NCA-Lys(Boc) was prepared by following the same procedure described in literatures (60% yield).[37] ^{1}H-NMR (400 MHz, Acetone) δ 7.97 (s, 1H), 5.99 (s, 1H), 4.56 (m, 1H), 3.10 (m, 2H), 1.88 (m, 2H), 1.55-1.38 (m, 13H). ^{13}C-NMR (101 MHz, Acetone) δ 171.9, 156.7, 152.9, 79.0, 58.5, 40.7, 32.4, 22.9.

NCA-Ala, 2. NCA-Ala was prepared by following the same procedure described in literatures (55% yield).[37] ^{1}H-NMR (400 MHz, Acetone) δ 7.88 (s, 1H), 4.59 (m, 1H), 1.49 (d, J = 8 Hz, 3H). ^{13}C-NMR (101 MHz, Acetone) δ 172.8, 152.6, 54.1, 17.8.

2.3 Polypeptide synthesis

Different molar ratios of 1 and 2 were dissolved in dry dimethyl formaldehyde (DMF) under dry argon at room temperature ([1]+[2] = 1.0 M). Hexamethyldisilazane (HMDS, 1 mol% of the total NCA monomers) was added into the above solution via syringe. The reaction was stirred for 24 h at rt, followed by the addition of water to get precipitates. The precipitates were filtered, washed with water, and dried under vacuum. The NMR spectral comparison of Intermediate-1 to -5 is summarized in Fig. S2 in the supporting information.

Intermediate-1, 88% yield. ^{1}H-NMR (400 MHz, DMSO) δ 9.05 (s, 100H), 6.78 (s, 100H), 4.41 (m, 100H), 2.88 (m, 200H), 1.68-1.35 (m, 1500H).

Intermediate-2, 85% yield. ^{1}H-NMR (400 MHz, DMSO) δ 9.05 (s, 100H), 6.77 (s, 80H), 4.39 (m, 100H), 2.87(m, 160H), 1.67-1.35 (m, 1260H).

Intermediate-3, 83% yield. ^{1}H-NMR (400 MHz, DMSO) δ 7.90 (s, 100H), 6.73 (s, 60H), 4.25 (b, 100H), 2.85 (b, 120H), 1.62-1.20 (m, 1020H).

Intermediate-4, 89% yield. ^{1}H-NMR (400 MHz, DMSO) δ 9.05 (s, 100H), 6.78 (s, 40H), 4.42 (m, 100H), 2.87 (m, 80H), 1.68-1.35 (m, 780H).

Intermediate-5, 91% yield. ^{1}H NMR (400 MHz, DMSO) δ 9.05 (s, 100H), 6.75 (s, 20H), 4.39 (m, 100H), 2.87 (m, 40H), 1.68-1.35 (m, 540H).

The *Boc* groups of polypeptides were removed by trifluoroacetic acid (TFA). Polypeptide (1 g) was dissolved in TFA (5 mL), and the solution was stirred for 2 h at rt. Half amount of TFA was evaporated by argon purging, and ethyl ether (30 mL) was added to get sticky precipitates. The above mixture was centrifuged, and the precipitates were washed with ethyl ether, dialyzed against DI water using a dialysis tubing (M. W. C. O. = 1000 Da), and freeze-dried under vacuum.

Polypeptide-1, 85% yield. ^{1}H-NMR (400 MHz, D$_2$O) δ 4.07 (m, 100H), 3.02 (m, 200H), 2.01-1.56 (600H).

Polypeptide-2, 90% yield. ^{1}H-NMR (400 MHz, D$_2$O) δ 4.07 (m, 100H), 3.00 (m, 160H), 2.01-1.54 (m, 480H).

Polypeptide-3, 88% yield. ^{1}H-NMR (400 MHz, D$_2$O) δ 4.25 (m, 100H), 2.99 (m, 120H), 1.92-1.37 (m, 360H).

Polypeptide-4, 87% yield. ^{1}H-NMR (400 MHz, D$_2$O) δ 4.06 (m, 100H), 3.04 (m, 80H), 2.00-1.52 (m, 240H).

Polypeptide-5, 85% yield. ^{1}H-NMR (400 MHz, DMSO) δ 4.35 (m, 100H), 3.12 (m, 40H), 2.10-1.69 (m, 120H).

2.4 PDI (Polydispersity Index) determination

The polymers (before flash column chromatography purification) were dissolved in THF (1 mg/mL). An aliquot (100 μL) of the polymer solution was injected and analyzed by Viscotek GPC system and OmniSEC software using a Phenogel column (300 × 7.80 mm, 5 μm, linear mixed bed, 0–75k MW range), and a RALS and RI dual detection system. Elution was performed at 0.5 mL/min with THF at 30 °C. In order to calculate the number-averaged molecular weight (M_n) and polydispersity index (PDI), a dn/dc value 0.12 ml/g was used for all polymers.

2.5 Preparation of crosslinked hydrogels

Hydrogels for all the bioassays were prepared in separate wells of 96-well or 48-well polystyrene plates. For a given well of 96-well plates, 35 μL of a polypeptide or trilysine stock solution was introduced, followed by the addition of 35 μL of a 6-arm PEG-ASG stock solution to initiate gelation. For a given well of 48-well plates, 50 μL of a polypeptide or trilysine stock solution was introduced, followed by the addition of 50 μL of a 6-arm PEG-ASG stock solution to initiate gelation. The resulting hydrogels were allowed to incubate at 37 °C for 2 h, followed by swelling in fresh DMEM (200 μL and 500 μL for 48-well and 96-well plates, respectively) overnight at 37 °C. Prior to the start of the assays, the media was aspirated.

2.6 Preparation of 3D collagen gels

Collagen gels for all the bioassays were prepared in separate wells of 48-well polystyrene plates. For a given well of 48-well plates, 100 μL of a collagen I (rat tail) stock solution (5 mg/mL, pH = 7.4) was introduced, and was incubated for 1 h at 37 °C to initiate gelation. The resulting hydrogels were allowed to incubate at 37 °C for 2 h, followed by swelling in fresh DMEM (500 μL) overnight at 37 °C. Prior to the start of the assays, the media was aspirated.

2.7 Rheometry characterization

Hydrogels were characterized using an AR-G2 rheometer (TA Instruments, New Castle, DE) with a 20 mm diameter parallel plate configuration. The evolution of storage (G') and loss (G'') moduli and phase angle (δ) at a constant strain of 0.05 was recorded as a function of frequency.

2.8 Live/Dead cell adhesion assay

Hydrogels were prepared in separate wells of 96-well plates. 3T3 cells in fresh media (~6K cells/well, 200 μL) were added on top of the hydrogels, and cultured for 96 h at 37 °C and 5% CO$_2$. The media was then aspirated, following by rinsing the hydrogel with 1×PBS

twice. A solution of LIVE/DEAD staining fluorescence dye (Ethidium Homodimer-1 (final 4 μM) and Calcein AM (final 2μM) in 1×PBS (100 μL)) was added to each well, and was incubated for 30 min at rt. The dye solution was removed by aspiration. Each hydrogel was rinsed with 1×PBS twice, and was covered with 1×PBS (100 μL) before imaging using an Zeiss Observer D.1 microscope. This assay was performed triplicately with two independent replicates.

2.9 MTT assay

Hydrogels were prepared in separate wells of 48-well plates. 3T3 cells in fresh media (~20K cells/well, 500 μL) were added on top of the hydrogels, and grown for 96 h at 37 °C and 5% CO_2. The media was aspirate, and each hydrogel was rinsed with 1×PBS twice. In each well, fresh media (300 μL) and a 12 mM MTT stock solution (30 μL) were introduced, and were incubated for 4 h at 37 °C. A SDS solution (300 μL) in 0.01 M HCl was mixed with the above MTT solution in each well thoroughly, and was incubated for 18 h at 37 °C. The supernatant was transferred to a blank well, and its UV absorbance at 570 nm was read on a BioTek Synergy 4 microplate reader. This assay was performed triplicately with two independent replicates.

2.10 PicoGreen cell proliferation assay

Hydrogels were prepared in separate wells of 48-well plates. 3T3 cells in fresh media (~20K cells/well, 500 μL) was added on top of the hydrogels, and cultured for 96 h at 37 °C and 5% CO_2. The media was then aspirate and each well was rinsed with 1×PBS twice followed by complete aspiration. Plates were stored for 24 h at −20°C for maximum cell lysis. A 1×TE buffer solution (250 μL) was added to each well, and was incubated for 30 min at rt, followed by shaking for 5 min at 300 rpm. Meanwhile, DNA standard solutions were prepared by diluting a 2 μg/mL DNA stock solution with 1×TE butter to make 50, 100, 200, 400, 600, 800 and 1000 ng/mL solutions (250 μL each). A PicoGreen reagent (250 μL) (200-fold dilution of the original stock PicoGreen reagent solution) was mixed with the above solution, and was shaken for 30 min at 300 rpm. The fluorescence ($\lambda_{Excitation}$ = 480 nm, $\lambda_{Emission}$ = 520 nm) of each solution was measured using a BioTek Synergy 4 microplate reader. This assay was performed triplicately with two independent replicates.

2.11 Antibacterial assay

Hydrogels were prepared in separate wells of 96-well plates. PEGDA gel was prepared from photopolymerization of a solution containing 70 μL 20 wt% sterile PEG-diacrylate (M.W. = 570) and 0.5 wt% (relative to the amount of PEGDA) of photoinitiator, 2,2-dimethoxy-2-phenylacetophenone under UV light (λ = 355 nm) for 20 min.[39] For each assay, 200 μL of the 5×10^7 CFU/mL bacterial stock solution in Tryptic Soy Broth (TSB) was introduced to the surface of a given hydrogel, and serial 1:10 dilutions were performed across the plate, resulting in final bacterial concentrations of 3.1×10^3, 3.1×10^4, 3.1×10^5, 3.1×10^6, 3.1×10^7, 3.1×10^8, and 3.1×10^9 CFU/dm² respectively, for each of seven wells. Controls were carried out on blank polystyrene surfaces. Bacteria were incubated on control and hydrogel surfaces for 48 h at 37 °C. Bacterial growth was monitored by measuring OD_{625nm} of the suspension above the gel. Corrected OD_{625nm} values were calculated according to the method described in the literature [28]. This assay was performed triplicately with two independent replicates.

3. Results

3.1 Preparation of polypeptides

Synthetic polypeptides can be prepared through ROP of α-amino acid NCAs [38, 40]. Primary alkyl amines under high vacuum [40], zerovalent nickel complexes [41–42], and HMDS [34] have been used to initiate living ROP reactions for the preparation of narrowly dispersed polypeptides. HMDS was chosen as the initiator since this metal-free initiator can generate polymers with better molecular weight control and lower PDIs than primary amines [34].

The route for synthesizing random copolypeptides is provided in Fig. 1. Random copolymers (Intermediate-1 to -5) containing varied molar ratios of Boc-protected lysine and alanine were synthesized through HMDS-mediated living ROP of NCA monomers 1 and 2 (Fig. 1). The structures of Intermediate-1 to Intermediate-5, contained ~100 subunits of amino acids as confirmed by ^{1}H-NMR analysis (Fig. S2). The deprotection of Boc-groups in the intermediate polymers using trifluoroacetic acid (TFA) yielded polypeptides Polypeptide-1 to -5 with varied hydrophobicity (Fig. 1). It is difficult to analyze the molecular weights and polydispersity indices (PDI) of the deprotected polypeptides (Polypeptide-1 to -5). Therefore, the molecular weights and PDIs of the intermediate polymers were characterized by gel permeation chromatography (GPC) using a right angle light scattering (RALS) and refractive index (RI) detection system. It is reasonable to expect that the deprotection of Boc- groups did not alter the length and composition of polypeptides. These random copolymers exhibited molecular weights close to their expected values (Table 1), and broad PDIs (1.8–1.9). The high PDIs of these polypeptides were caused by the interference of shoulders on the low M_n side in the GPC traces (data not shown). These shoulders may arise from degradation of an active propagating polymer chain in air or moisture [34].

3.2 Hydrogel formation

Fast coupling between amines and *N*-hydroxysuccinimide (NHS) esters in neutral aqueous media has proved efficient in many biomedical applications [43–46]. In the presented work, we created hydrogels via cross-linking polypeptides bearing amine groups with multi-arm NHS ester terminated PEG. PEG has been used for numerous drug delivery [47–52] and tissue engineering [53–57] applications due to its many useful characteristics such as protein resistance, biocompatibility, minimal toxicity and immunogenicity, and high solubility in water. In addition, we utilized PEG in this study for its inert properties, as it would allow us to specifically study and control the addition of bioactive components. Therefore, 6-arm PEG-ASG (M_w = 10K) was chosen as the cross-linker for the polypeptides.

To make chemically cross-linked hydrogels, polypeptides and 6-arm PEG-ASG (M_w = 10K) were dissolved in separate PBS buffer solutions with varied pH values and weight percentages (Table 2). To slow down the degradation of 6-arm PEG-ASG in aqueous solution, 6-arm PEG-ASG was dissolved in acidic PBS buffer solution (pH = 4). Equal volumes of polypeptide and PEG solutions were mixed to form the hydrogels, with the final mixtures being neutral (Fig. 2). Optimized gelation conditions for trilysine or polypeptides are summarized in Table 2. Gels were formed within 5 min at rt.

3.3 Cell adhesion and proliferation

To evaluate the ability of the polypeptide hydrogels to support cell adhesion, NIH 3T3 fibroblasts, an immortalized cell type commonly used in adhesion and proliferation experiments [58], were used. Fibroblasts were seeded on these hydrogels (Gel-I to Gel-VI)

and cultured for four days; cell viability was evaluated using a LIVE/DEAD assay (Fig. 3). Only Gel-III & IV supported cell adhesion.

Mitochondrial activities of fibroblasts on the above hydrogel surfaces after 4 days in culture were measured and compared with that on collagen gels using a MTT assay kit (Fig. 4). Fibroblasts cultured on Gel-III exhibited higher mitochondrial activity than those on Gel-IV, which is consistent with our cell adhesion results (Fig. 3). As expected, due to inadequate cell adhesion, metabolic activity on the other gels (Gel-I & II, Gel-V & VI) was unchanged over the blank control wells (Fig. 4). Fibroblasts on collagen gels showed higher metabolic activity than those on the other hydrogels (Gel-I to -VI).

The ability of Gel–III and -IV to support cell proliferation was assessed using a PicoGreen assay. After four days in culture, cell proliferation on Gel-III was significantly greater than that on Gel-VI (Fig. 5). As expected from the MTT assay, cell proliferation on the synthetic gels was significantly lower than proliferation on collagen gels. It has been shown that many synthetic polymers have reduced cell adhesion and proliferation compared to natural ECM components, such as collagen, since they contain limited biological signals [6].

3.4 Antibacterial activities

The bacterial proliferation on Gel-III, which was formed by cross-linking Polypeptide-3 and 6-arm PEG-ASG, was quantified by measuring the optical density (OD) at 625 nm of the supernatant after incubation at 37 °C for 18 h (Fig. 6). This method, in which the OD readings indicate the amount of both live and dead bacteria, has been previously established for characterization of the antibacterial activity of a hydrogel by Schneider et al. [28]. The OD results from Gel-III were compared with two positive controls for bacterial growth: the PEGDA gel (no antibacterial activity) and incubation without any hydrogel (blank control). While Polypeptide-3 in solution did not inhibit bacterial growth (Fig. S3), Gel-III was capable of efficiently inhibiting both *E. coli* JM109 and *S. aureus* ATCC25923 growth when a bacterial density of up to 3.1×10^9 CFU/dm^2 was initially seeded on the hydrogel (the bacterial density was calculated by dividing the initial bacterial CFUs by the bottom surface area of wells in the tissue culture plate), as compared to non-coated polystyrene plates (Fig. 6).

3.5 Rheology

To assess the mechanical properties of the potential wound healing scaffolds, rheological properties of Gel-III, Gel-VI and PEGDA gel were compared in Fig. 7. The data obtained for all gels was characterized by storage (G') and loss stimuliG''), both exhibiting a plateau in the frequency range studied. Gel-VI ($G' = 3000$ Pa at 1 Hz) was around 2-fold stiffer than Gel-III ($G' = 1400$ Pa at 1 Hz), while both gels were more compliant than the PEGDA gel (6310 Pa at 1 Hz). Collagen-based hydrogels have been used extensively in wound healing, [5–6] and their typical G' (around 78 Pa at 1Hz, collagen = 1.6 mg/mL)[59] is much lower than that of Gel-III.

4. Discussion

4.1 Cell adhesion and proliferation

Among the synthetic gels (Table 2), only Gel-III & IV exhibited cell adhesion activities. The cell adhesion properties of Gel-III & IV are likely a result of a higher weight percentage of polypeptides (5 wt%), as PEG is well known to be both protein and cell resistant when its molecular weight is above 2000 Da [60–64]. Due to the poor water solubility of Polypeptide-5 (Table 2), many undissolved Polypeptide-5 solid aggregates were encapsulated inside Gel-V. Therefore, the actual weight percentage of Polypeptide-5 in the

components of Gel-V was much lower than the theoretical value (5 wt%), which likely resulted in the inability of Gel-V to support cell adhesion. Fibroblasts maintained a more characteristic morphology on Gel-III. While the cells were attached to Gel-IV, the cells had a rounded morphology, indicating weak cell adhesion. The difference in cell spreading morphology between Gel-III and Gel-IV may be due to the different amphiphilicity of Polypeptide-3 and Polypeptide-4. It has been shown that cell adhesion can be inhibited by materials at the extremes of hydrophilicity or hydrophobicity [65–67]. Our data demonstrates that, out of the hydrogels tested, Gel-III composed of Polypeptide-3 and 6-arm PEG-ASG exhibited the best cationic/hydrophobic balance for cell adhesion.

Previous studies have shown that collagen, the most abundant extracellular matrix (ECM) protein, promotes cell adhesion, migration and proliferation better than many synthetic polymeric matrices [68–70]. It is also known that PEG with higher molecular weights conjugate with biomaterials to reduce protein and cell adhesion due to the nonfouling property of PEG surfaces [68, 71–74]. Therefore, it is reasonable that our polypeptide-PEG hydrogels displayed lower metabolic activity than a purely collagen gel (Fig. 4 & 5). Our data also suggests that reduction in weight percentage ratio of PEG in the polypeptide-PEG hydrogels may facilitate increasing their cell adhesion and metabolic activities.

4.2 Antibacterial activities

The cell adhesion and proliferation results indicated that Gel-III was the most promising scaffold for wound healing among the above polypeptide hydrogels. Therefore, Gel-III was selected to test its antibacterial activity against *E. coli* JM109 and *S. aureus* ATCC25923. The seeding bacterial suspensions with varied concentrations (5×10^2, 5×10^3, 5×10^4, 5×10^4, 5×10^5, 5×10^6, and 5×10^7 CFU/mL respectively) were added on top of hydrogels. If bacterial growth was not inhibited, the final OD readings after 48h were expected to be around $0.2 - 1.3$, which was confirmed by the PEGDA gel control and blank control (Fig. 6). The final OD data for Gel-III were around 0, which demonstrates that bacterial growth was inhibited efficiently when a bacterial density of up to 3.1×10^9 CFU/dm^2 was initially seeded on the hydrogel. During formation of Gel-III, the amount of amine groups in Polypeptide-3 was around 10–20% more than that of N-hydroxysuccinimide (NHS) groups in 6-arm PEG-ASG. Therefore, based on the assumption that NHS groups can completely react with amines in polypeptides, after cross-linking, around 80–90% of amine groups in Polypeptide-3 could be converted to amide groups, which greatly decreased the hydrophilicity of polypeptide itself. Meanwhile, around 10–20% of unreacted amine groups should remain in Gel-III. As a result, the polypeptide component in Gel-III likely maintained an adequate cationic/hydrophobic balance to inhibit bacterial growth (Fig. 8). The concentration of PEG crosslinker (16 wt%, Table 2) for the presented experiments was chosen as the optimal value to achieve both gelation and support antibacterial activities. A lower PEG concentration resulted in no gelation, while a higher PEG concentration led to loss of antibacterial activities of the gel (data not shown), which was likely a result of too few amine groups left to kill the bacteria. In preliminary experiments, we also examined the use of a linear 2-arm PEG NHS ester crosslinker in addition to the 6-arm PEG-ASG presented here; however, no gel was formed with concentrations up to 20 wt% (data not shown). One possible explanation is that the 3D network formed by crosslinking with 6-arm PEG is denser than that formed by 2-arm PEG. In addition the degradation properties of PEG-NHS esters could have contributed to this effect as it is well known that the hydrolysis of PEG-NHS esters is very rapid in a neutral pH solution and hydrolysis of only one NHS ester in the 2-arm PEG would prevent crosslinking. As a result, 6-arm PEG is a more robust crosslinker for gelation and was chosen for our experiments.

It has been reported that poly(Lys-Ala) polypeptides killed bacteria efficiently through membrane disruption [75]. The rapid interaction between bacterial membranes and AMP

mimics (Fig. 8) would cause membrane depolarization [76], potassium release[76] or pore formation [76], which would finally lead to cell death. Most mammalian cells, on the other hand, are richer in the neutral phospholipids (such as phosphatidylcholine) and cholesterol, which would lead to weaker electrostatic interactions between these cells and Gel-III. After cross-linking, polypeptides in Gel-III likely maintained a more rigid conformation which is thought to be preferred for killing bacteria [77–80]. It has been shown that conformationally restrained arylamide or phenylene ethynylene oligomers exhibited much better antimicrobial activities than other AMP mimics [77–80]. An antimicrobial hydrogel based on the crosslinking between an AMP mimic and biocompatible chitosan was recently reported; it was suggested that the antibacterial properties are facilitated by the nanoporous structure of the gel [81]. Likewise, bacteria are likely interacting within the pores of Gel-III in addition to its surface, causing enhanced bacterial membrane disruption.

Although PEG surfaces have little adhesion of proteins, they are not necessarily resistant to bacterial adhesion [82]. To further demonstrate that the PEG component in Gel-III did not act as an antibiotic, the bacterial growth above the PEGDA ($M_w = 570$) gel was also monitored (Fig. 6). As expected, bacteria proliferated successfully on the PEGDA gel, which suggests that the free amine groups instead of the PEG component in Gel-III likely serve as antibacterial agents.

4.3 Gel-III vs Collagen

An additional reason collagen has been well studied in wound healing is that collagenous fibers are the major component of scar tissue in the final step of wound repair [5]. Forms of collagen wound dressings can be classified as hydrogels [83], sponges [69], and films [84]. Many commercial collagen-based wound dressings have already been developed, such as Nu-Gel® (Johnson & Johnson), CellerateRX® (A Wound Management Technologies, Inc.), Puracol Plus® (Medline Industries, Inc), or Biostep® and Biostep Ag® (Smith & Nephew).

A disadvantage of collagen hydrogels is their low mechanical properties [83]. Collagen sponges and lattices with stronger mechanical properties have been prepared for wound repair; however, they still showed poor *in vivo* stability [85–86]. Our polypeptide-PEG gel Gel-III is much stronger than collagen gels as measured by rheology (Fig. 7), and thus, may provide more adequate mechanical support for wound healing. Furthermore, Gel-III is likely more stable than collagen gels both *in vivo* and *in vitro* due to its dense chemically cross-linking network (Fig. 2).

Application of collagen wound dressings also requires sterilization or incorporation of antibiotics [5]. Other concerns include their high cost, immunogenicity, and lot-to-lot variability of physiochemical and degradation properties [87–88]. Our synthetic hydrogel Gel-III can likely overcome these concerns due to its low cost, inherent antibacterial activity, and high batch-to-batch consistency.

5. Conclusion

In conclusion, we prepared an easily-synthesized cell-adhesive hydrogel Gel-III with inherent antibacterial activity. Our data suggest that higher weight ratios between polypeptide and PEG in the hydrogel composition are better for cell adhesion and proliferation. In this study, both the antibacterial and cell adhesion properties were modulated through the addition of the polypeptides. Further studies are, however, underway to enhance cell adhesion through the incorporation of additional biological moeities. We expect that these novel hydrogels will have potential applications in wound healing. In addition to their inherent antibacterial activity, easy synthesis, and high batch-to-batch consistency, these polypeptide hydrogels should also allow for facile tethering of bioactive

moieties [89–90], which could further enhance cell adhesion and proliferation, and accelerate wound healing.

Supplementary Material

Refer to Web version on PubMed Central for supplementary material.

Acknowledgments

References

[1]. Rizzi SC, Upton Z, Bott K, Dargaville TR. Recent advances in dermal wound healing: biomedical device approaches. Expert Rev Med Dev. 2010; 7:143–54.

[2]. Bello YM, Phillips TJ. Recent advances in wound healing. J Am Med Assoc. 2000; 283:716–8.

[3]. Doherty, GM. Current diagnosis and treatment surgery. 13th ed. McGrwa-Hill Companies; 2010. p. 53-4.

[4]. Ovington LG. Advances in wound dressings. Clin Dermatol. 2007; 25:33–8. [PubMed: 17276199]

[5]. Purna SK, Babu M. Collagen based dressings--a review. Burns. 2000; 26:54–62. [PubMed: 10630321]

[6]. Zhong SP, Zhang YZ, Lim CT. Tissue scaffolds for skin wound healing and dermal reconstruction. Wiley Interdiscip Rev Nanomed Nanobiotechnol. 2010; 2:510–25. [PubMed: 20607703]

[7]. Robson MC, Krizek TJ, Koss N, Samburg JL. Amniotic Membranes as a Temporary Wound Dressing. Surg Gynecol Obstet. 1973; 136:904–6. [PubMed: 4703471]

[8]. Unger MG, Roberts M. Lyophilized Amniotic Membranes on Graft Donor Sites. Brit J Plast Surg. 1976; 29:99–101. [PubMed: 773479]

[9]. Kim ZW, Kron S, Arumugam S, Hoff A, Enquist IF. The Effect of Homograft Rejection on Wound Healing. Surg Gynecol Obstetr. 1970; 131:495–9.

[10]. Yannas IV, Burke JF, Warpehoski M, Stasikelis P, Skrabut EM, Orgill D, et al. Prompt, Long-Term Functional Replacement of Skin. Trans Am Soc Art Int Org. 1981; 27:19–23.

[11]. Sun WQ, Gouk SS. Aging of a Regenerative Biologic Scaffold (AlloDerm Native Tissue Matrix) During Storage at Elevated Humidity and Temperature. Tiss Eng Part C-Methods. 2009; 15:23–31.

[12]. Geiger M, Li RH, Friess W. Collagen sponges for bone regeneration with rhBMP-2. Adv Drug Deliv Rev. 2003; 55:1613–29. [PubMed: 14623404]

[13]. Price RD, Berry MG, Navsaria HA. Hyaluronic acid: the scientific and clinical evidence. J Plastic Reconstruct Aesthetic Surg. 2007; 60:1110–9.

[14]. Harris PA, di Francesco F, Barisoni D, Leigh IM, Navsaria HA. Use of hyaluronic acid and cultured autologous keratinocytes and fibroblasts in extensive burns. Lancet. 1999; 353:35–6. [PubMed: 10023951]

[15]. Hollander DA, Soranzo C, Falk S, Windolf J. Extensive traumatic soft tissue loss: Reconstruction in severely injured patients using cultured hyaluronan-based three-dimensional dermal and epidermal autografts. J Trauma. 2001; 50:1125–36. [PubMed: 11426129]

[16]. Ma J, Wang H, He B, Chen J. A preliminary in vitro study on the fabrication and tissue engineering applications of a novel chitosan bilayer material as a scaffold of human neofetal dermal fibroblasts. Biomaterials. 2001; 22:331–6. [PubMed: 11205436]

[17]. Horn MM, Martins VCA, Plepis AMD. Interaction of anionic collagen with chitosan: Effect on thermal and morphological characteristics. Carbohyd Polym. 2009; 77:239–43.

[18]. Murakami K, Aoki H, Nakamura S, Nakamura S, Takikawa M, Hanzawa M, et al. Hydrogel blends of chitin/chitosan, fucoidan and alginate as healing-impaired wound dressings. Biomaterials. 2010; 31:83–90. [PubMed: 19775748]

[19]. Chua AWC, Ma DR, Song IC, Phan TT, Lee ST, Song C. In vitro evaluation of fibrin mat and Tegaderm (TM) wound dressing for the delivery of keratinocytes - Implications of their use to treat burns. Burns. 2008; 34:175–80. [PubMed: 18029101]

[20]. Chen GP, Sato T, Ohgushi H, Ushida T, Tateishi T, Tanaka J. Culturing of skin fibroblasts in a thin PLGA-collagen hybrid mesh. Biomaterials. 2005; 26:2559–66. [PubMed: 15585258]

[21]. Beumer GJ, van Blitterswijk CA, Bakker D, Ponec M. Cell-seeding and in vitro biocompatibility evaluation of polymeric matrices of PEO/PBT copolymers and PLLA. Biomaterials. 1993; 14:598–604. [PubMed: 8399953]

[22]. Dai NT, Williamson MR, Khammo N, Adams EF, Coombes AGA. Composite cell support membranes based on collagen and polycaprolactone for tissue engineering of skin. Biomaterials. 2004; 25:4263–71. [PubMed: 15046916]

[23]. Schneider A, Garlick JA, Egles C. Self-assembling peptide nanofiber scaffolds accelerate wound healing. PLoS One. 2008; 3:e1410. [PubMed: 18183291]

[24]. Queen D, Orsted H, Sanada H, Sussman G. A dressing history. Int Wound J. 2004; 1:59–77. [PubMed: 16722898]

[25]. Ito T, Fraser IP, Yeo Y, Highley CB, Bellas E, Kohane DS. Anti-inflammatory function of an in situ cross-linkable conjugate hydrogel of hyaluronic acid and dexamethasone. Biomaterials. 2007; 28:1778–86. [PubMed: 17204321]

[26]. Obara K, Ishihara M, Ishizuka T, Fujita M, Ozeki Y, Maehara T, et al. Photocrosslinkable chitosan hydrogel containing fibroblast growth factor-2 stimulates wound healing in healing-impaired db/db mice. Biomaterials. 2003; 24:3437–44. [PubMed: 12809772]

[27]. Luo Y, Diao H, Xia S, Dong L, Chen J, Zhang J. A physiologically active polysaccharide hydrogel promotes wound healing. J Biomed Mater Res. 2010; 94:193–204.

[28]. Salick DA, Kretsinger JK, Pochan DJ, Schneider JP. Inherent antibacterial activity of a peptide-based beta-hairpin hydrogel. J Am Chem Soc. 2007; 129:14793–9. [PubMed: 17985907]

[29]. Kenawy ER, Worley SD, Broughton R. The chemistry and applications of antimicrobial polymers: A state-ofthe-art review. Biomacromolecules. 2007; 8:1359–84. [PubMed: 17425365]

[30]. Worley SD, Sun G. Biocidal polymers. Trends Polym Sci. 1996; 4:364–70.

[31]. Yu HJ, Xu XY, Chen XS, Lu TC, Zhang PB, Jing XB. Preparation and antibacterial effects of PVA-PVP hydrogels containing silver nanoparticles. J Appl Polym Sci. 2007; 103:125–33.

[32]. Rattanaruengsrikul V, Pimpha N, Supaphol P. Development of Gelatin Hydrogel Pads as Antibacterial Wound Dressings. Macromol Biosci. 2009; 9:1004–15. [PubMed: 19530128]

[33]. Brogden KA. Antimicrobial peptides: pore formers or metabolic inhibitors in bacteria? Nat Rev Microbiol. 2005; 3:238–50. [PubMed: 15703760]

[34]. Lu H, Cheng JJ. Hexamethyldisilazane-mediated controlled polymerization of alpha-Amino acid N-carboxyanhydrides. J Am Chem Soc. 2007; 129:14114–5. [PubMed: 17963385]

[35]. Yount NY, Bayer AS, Xiong YQ, Yeaman MR. Advances in antimicrobial peptide immunobiology. Biopolymers. 2006; 84:435–58. [PubMed: 16736494]

[36]. Schneider T, Kruse T, Wimmer R, Wiedemann I, Sass V, Pag U, et al. Plectasin, a fungal defensin, targets the bacterial cell wall precursor Lipid II. Science. 2010; 328:1168–72. [PubMed: 20508130]

[37]. Habraken GJM, Peeters M, Dietz CHJT, Koning CE, Heise A. How controlled and versatile is N-carboxy anhydride (NCA) polymerization at 0 degrees C? Effect of temperature on homo-, block- and graft (co)polymerization. Polymer Chem. 2010; 1:514–24.

[38]. Deming TJ. Synthetic polypeptides for biomedical applications. Prog Polym Sci. 2007; 32:858–75.

[39]. Tan GX, Wang YJ, Li J, Zhang SJ. Synthesis and characterization of injectable photocrosslinking poly (ethylene glycol) diacrylate based hydrogels. Polym Bull. 2008; 61:91–8.

[40]. Aliferis T, Iatrou H, Hadjichristidis N. Living polypeptides. Biomacromolecules. 2004; 5:1653–6. [PubMed: 15360270]

[41]. Nowak AP, Breedveld V, Pakstis L, Ozbas B, Pine DJ, Pochan D, et al. Rapidly recovering hydrogel scaffolds from self-assembling diblock copolypeptide amphiphiles. Nature. 2002; 417:424–8. [PubMed: 12024209]

[42]. Yang CY, Song B, Ao Y, Nowak AP, Abelowitz RB, Korsak RA, et al. Biocompatibility of amphiphilic diblock copolypeptide hydrogels in the central nervous system. Biomaterials. 2009; 30:2881–98. [PubMed: 19251318]

[43]. Pieper JS, Hafmans T, Veerkamp JH, van Kuppevelt TH. Development of tailor-made collagen-glycosaminoglycan matrices: EDC/NHS crosslinking, and ultrastructural aspects. Biomaterials. 2000; 21:581–93. [PubMed: 10701459]

[44]. Kuijpers AJ, Engbers GH, Krijgsveld J, Zaat SA, Dankert J, Feijen J. Cross-linking and characterisation of gelatin matrices for biomedical applications. J Biomater Sci Polym Ed. 2000; 11:225–43. [PubMed: 10841277]

[45]. Wissink MJ, Beernink R, Pieper JS, Poot AA, Engbers GH, Beugeling T, et al. Immobilization of heparin to EDC/NHS-crosslinked collagen. Characterization and in vitro evaluation. Biomaterials. 2001; 22:151–63. [PubMed: 11101159]

[46]. Chua PH, Neoh KG, Shi Z, Kang ET. Structural stability and bioapplicability assessment of hyaluronic acid-chitosan polyelectrolyte multilayers on titanium substrates. J Biomed Mater Res. 2008; 87:1061–74.

[47]. Gou M, Gong C, Zhang J, Wang X, Gu Y, Guo G, et al. Polymeric matrix for drug delivery: honokiol-loaded PCL-PEG-PCL nanoparticles in PEG-PCL-PEG thermosensitive hydrogel. J Biomed Mater Res. 2010; 93:219–26.

[48]. Bhirde AA, Patel S, Sousa AA, Patel V, Molinolo AA, Ji Y, et al. Distribution and clearance of PEG-single-walled carbon nanotube cancer drug delivery vehicles in mice. Nanomedicine. 2010; 5:1535–46. [PubMed: 21143032]

[49]. Chen FH, Zhang LM, Chen QT, Zhang Y, Zhang ZJ. Synthesis of a novel magnetic drug delivery system composed of doxorubicin-conjugated Fe_3O_4 nanoparticle cores and a PEG-functionalized porous silica shell. Chem Commun. 2010; 46:8633–5.

[50]. Chang G, Li C, Lu W, Ding J. N-Boc-histidine-capped PLGA-PEG-PLGA as a smart polymer for drug delivery sensitive to tumor extracellular pH. Macromol Biosci. 2010; 10:1248–56. [PubMed: 20593367]

[51]. Mei H, Shi W, Pang Z, Wang H, Lu W, Jiang X, et al. EGFP-EGF1 protein-conjugated PEG-PLA nanoparticles for tissue factor targeted drug delivery. Biomaterials. 2010; 31:5619–26. [PubMed: 20413154]

[52]. Wang H, Zhao P, Liang X, Gong X, Song T, Niu R, et al. Folate-PEG coated cationic modified chitosan--cholesterol liposomes for tumor-targeted drug delivery. Biomaterials. 2010; 31:4129–38. [PubMed: 20163853]

[53]. Zhang M, Li XH, Gong YD, Zhao NM, Zhang XF. Properties and biocompatibility of chitosan films modified by blending with PEG. Biomaterials. 2002; 23:2641–8. [PubMed: 12059013]

[54]. Hou Y, Schoener CA, Regan KR, Munoz-Pinto D, Hahn MS, Grunlan MA. Photo-cross-linked PDMSstar-PEG hydrogels: synthesis, characterization, and potential application for tissue engineering scaffolds. Biomacromolecules. 2010; 11:648–56. [PubMed: 20146518]

[55]. Tan H, DeFail AJ, Rubin JP, Chu CR, Marra KG. Novel multiarm PEG-based hydrogels for tissue engineering. J Biomed Mater Res. 2010; 92:979–87.

[56]. Rafat M, Li F, Fagerholm P, Lagali NS, Watsky MA, Munger R, et al. PEG-stabilized carbodiimide crosslinked collagen-chitosan hydrogels for corneal tissue engineering. Biomaterials. 2008; 29:3960–72. [PubMed: 18639928]

[57]. Burdick JA, Anseth KS. Photoencapsulation of osteoblasts in injectable RGD-modified PEG hydrogels for bone tissue engineering. Biomaterials. 2002; 23:4315–23. [PubMed: 12219821]

[58]. Webb K, Hlady V, Tresco PA. Relative importance of surface wettability and charged functional groups on NIH 3T3 fibroblast attachment, spreading, and cytoskeletal organization. J Biomed Mater Res. 1998; 41:422–30. [PubMed: 9659612]

[59]. Tan J, Saltzman WM. Influence of synthetic polymers on neutrophil migration in three-dimensional collagen gels. J Biomed Mater Res. 1999; 46:465–74. [PubMed: 10398007]

[60]. Hern DL, Hubbell JA. Incorporation of adhesion peptides into nonadhesive hydrogels useful for tissue resurfacing. J Biomed Mater Res. 1998; 39:266–76. [PubMed: 9457557]

[61]. Gonzalez AL, Gobin AS, West JL, McIntire LV, Smith CW. Integrin interactions with immobilized peptides in polyethylene glycol diacrylate hydrogels. Tissue Eng. 2004; 10:1775–86. [PubMed: 15684686]

[62]. Lee JH, Lee HB, Andrade JD. Blood compatibility of polyethylene oxide surfaces. Prog Polym Sci. 1995; 20:1043–79.

[63]. Dumitrium, S. Polymeric Biomaterials, Revised and Expanded. CRC Press; New York: 2001.

[64]. Ratner, BD.; Hoffman, AS.; Schoen, FJ.; Lemons, JE. Biomaterials science: an introduction to materials in medicine. Elsevier Academic Prss; San Diego: 2004.

[65]. Wilson CJ, Clegg RE, Leavesley DI, Pearcy MJ. Mediation of biomaterial-cell interactions by adsorbed proteins: a review. Tissue Eng. 2005; 11:1–18. [PubMed: 15738657]

[66]. Alves NM, Shi J, Oramas E, Santos JL, Tomas H, Mano JF. Bioinspired superhydrophobic poly(L-lactic acid) surfaces control bone marrow derived cells adhesion and proliferation. J Biomed Mater Res. 2009; 91:480–8.

[67]. Kim SH, Ha HJ, Ko YK, Yoon SJ, Rhee JM, Kim MS, et al. Correlation of proliferation, morphology and biological responses of fibroblasts on LDPE with different surface wettability. J Biomater Sci Polym Ed. 2007; 18:609–22. [PubMed: 17550662]

[68]. Tan J, Saltzman WM. Influence of synthetic polymers on neutrophil migration in three-dimensional collagen gels. J Biomed Mater Res. 1999; 46:465–74. [PubMed: 10398007]

[69]. Doillon CJ. Porous collagen sponge wound dressings: in vivo and in vitro studies. J Biomater Appl. 1988; 2:562–78. [PubMed: 3058927]

[70]. Doillon CJ, Whyne CF, Brandwein S, Silver FH. Collagen-based wound dressings: control of the pore structure and morphology. J Biomed Mater Res. 1986; 20:1219–28. [PubMed: 3782179]

[71]. Zalipsky S, Harris JM. Introduction to chemistry and biological applications of poly(ethylene glycol). Acs Sym Ser. 1997; 680:1–13.

[72]. Llanos GR, Sefton MV. Does Polyethylene Oxide Possess a Low Thrombogenicity. J Biomater Sci Polym Ed. 1993; 4:381–400. [PubMed: 8373752]

[73]. Drumheller PD, Hubbell JA. Densely crosslinked polymer networks of poly(ethylene glycol) in trimethylolpropane triacrylate for cell-adhesion-resistant surfaces. J Biomed Mater Res. 1995; 29:207–15. [PubMed: 7738068]

[74]. Du H, Chandaroy P, Hui SW. Grafted poly-(ethylene glycol) on lipid surfaces inhibits protein adsorption and cell adhesion. Biochim Biophys Acta. 1997; 1326:236–48. [PubMed: 9218554]

[75]. Zhou C, Qi X, Li P, Chen WN, Mouad L, Chang MW, et al. High potency and broad-spectrum antimicrobial peptides synthesized via ring-opening polymerization of alpha-aminoacid-N-carboxyanhydrides. Biomacromolecules. 2010; 11:60–7. [PubMed: 19957992]

[76]. Song A, Walker SG, Parker KA, Sampson NS. Antibacterial Studies of Cationic Polymers with Alternating, Random, and Uniform Backbones. ACS Chem Biol. 2011

[77]. Scott RW, DeGrado WF, Tew GN. De novo designed synthetic mimics of antimicrobial peptides. Curr Opin Biotechnol. 2008; 19:620–7. [PubMed: 18996193]

[78]. Choi S, Isaacs A, Clements D, Liu D, Kim H, Scott RW, et al. De novo design and in vivo activity of conformationally restrained antimicrobial arylamide foldamers. Proc Natl Acad Sci. 2009; 106:6968–73. [PubMed: 19359494]

[79]. Yang L, Gordon VD, Mishra A, Som A, Purdy KR, Davis MA, et al. Synthetic antimicrobial oligomers induce a composition-dependent topological transition in membranes. J Am Chem Soc. 2007; 129:12141–7. [PubMed: 17880067]

[80]. Tew GN, Scott RW, Klein ML, Degrado WF. De novo design of antimicrobial polymers, foldamers, and small molecules: from discovery to practical applications. Acc Chem Res. 2010; 43:30–9. [PubMed: 19813703]

[81]. Li P, Poon YF, Li W, Zhu HY, Yeap SH, Cao Y, et al. A polycationic antimicrobial and biocompatible hydrogel with microbe membrane suctioning ability. Nat Mater. 2011; 10:149–56. [PubMed: 21151166]

[82]. Wei J, Ravn DB, Gram L, Kingshott P. Stainless steel modified with poly(ethylene glycol) can prevent protein adsorption but not bacterial adhesion Colloids Surf, B. 2003; 32:275–91.

[83]. Auger FA, Rouabhia M, Goulet F, Berthod F, Moulin V, Germain L. Tissue-engineered human skin substitutes developed from collagen-populated hydrated gels: clinical and fundamental applications. Med Biol Eng Comput. 1998; 36:801–12. [PubMed: 10367474]

[84]. Shettigar UR, Jagannathan R, Natarajan R. Collagen film for burn wound dressings reconstituted from animal intestines. Artif Organs. 1982; 6:256–60. [PubMed: 7181726]

[85]. Ono I, Tateshita T, Inoue M. Effects of a collagen matrix containing basic fibroblast growth factor on wound contraction. J Biomed Mater Res. 1999; 48:621–30. [PubMed: 10490675]

[86]. Berry DP, Harding KG, Stanton MR, Jasani B, Ehrlich HP. Human wound contraction: collagen organization, fibroblasts, and myofibroblasts. Plast Reconstr Surg. 1998; 102:124–31. [PubMed: 9655417]

[87]. Peng YY, Glattauer V, Ramshaw JA, Werkmeister JA. Evaluation of the immunogenicity and cell compatibility of avian collagen for biomedical applications. J Biomed Mater Res. 2010; 93:1235–44.

[88]. Lee CH, Singla A, Lee Y. Biomedical applications of collagen. Int J Pharm. 2001; 221:1–22. [PubMed: 11397563]

[89]. Sun J, Schlaad H. Thiol-ene clickable polypeptides. Macromolecules. 2010; 43:4445–8.

[90]. Engler AC, Lee HI, Hammond PT. Highly Efficient "Grafting onto" a Polypeptide Backbone Using Click Chemistry. Angew Chem Int Ed. 2009; 48:9334–8.
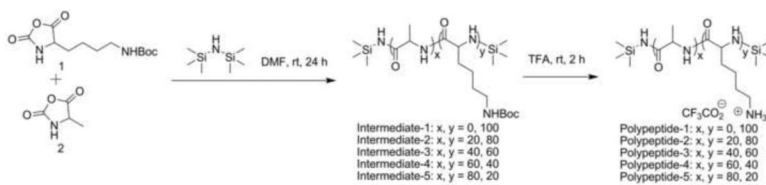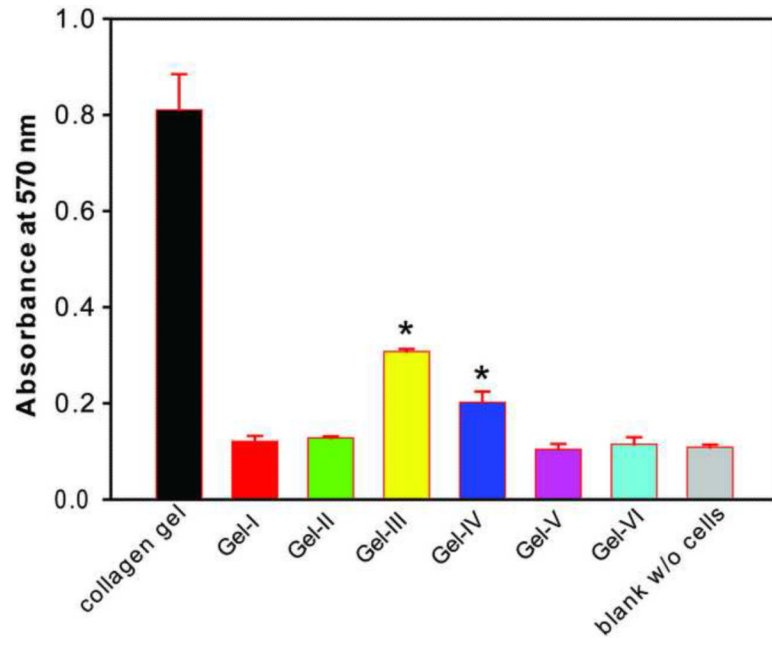
Fig. 1.
Synthesis of polypeptides (Polypeptide-1 to -5). [1]+[2] = 1.0 M.
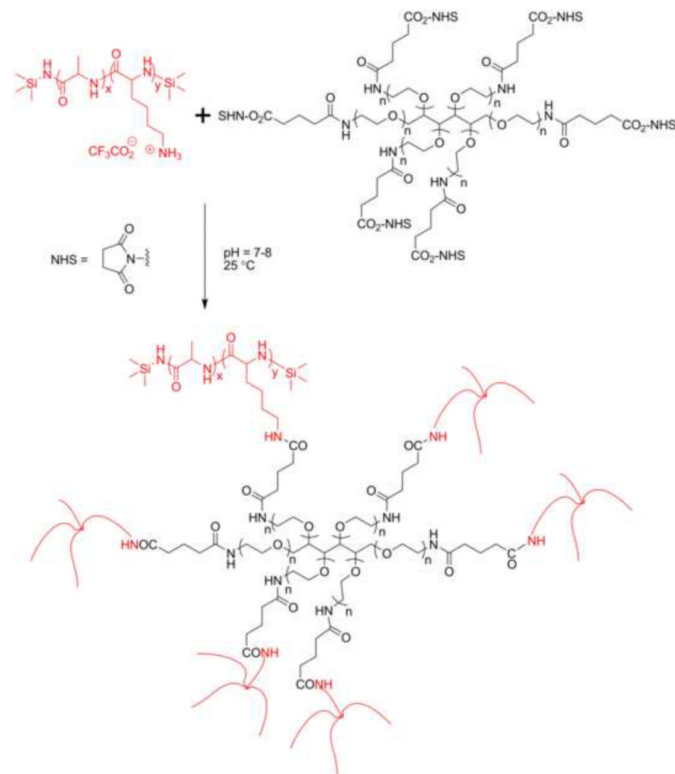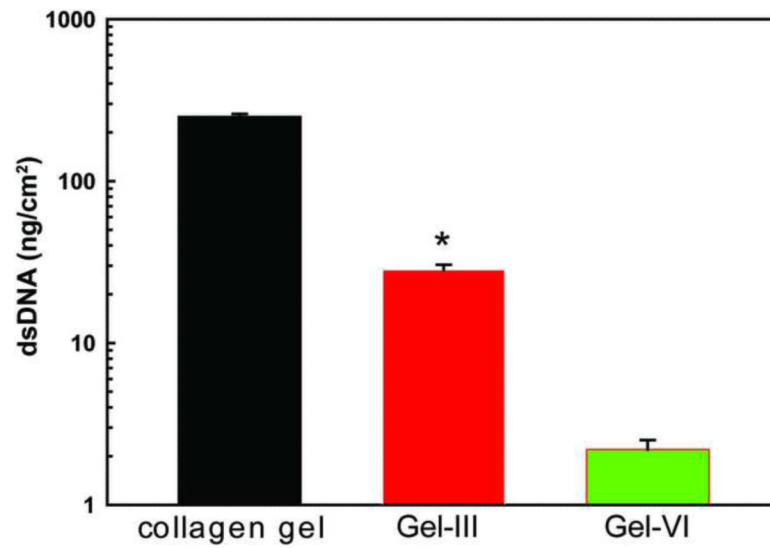
Fig. 2.
Crosslinking between polypeptides and 6-arm PEG-ASG in PBS buffer (final pH = 7) at 25 °C.
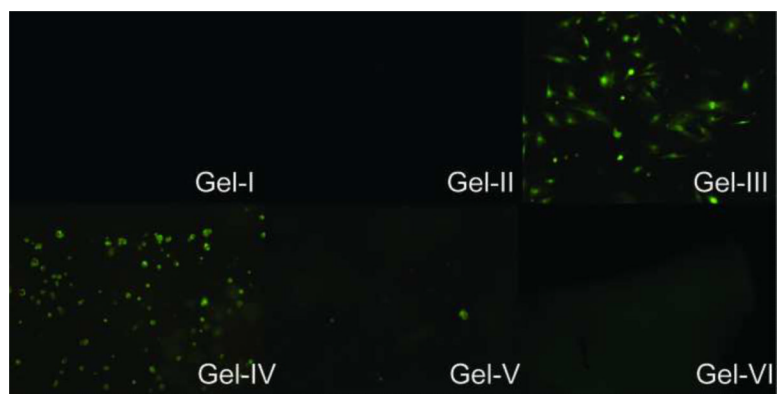
Fig. 3.
Photomicrographs of live/dead 3T3 fibroblasts adhered to hydrogels after four days in culture.

Fig. 4.
Mitochondrial activity of 3T3 cells on different surfaces after four days in culture. * $p < 0.01$ compared to Gel-VI.

Fig. 5.
Proliferation of fibroblasts on collagen 3D gel (■), Gel-III (■) and Gel-VI (■) after four days in culture, as measured by DNA contents of cells bound to hydrogels. * *p* < 0.01 compared to Gel-VI.
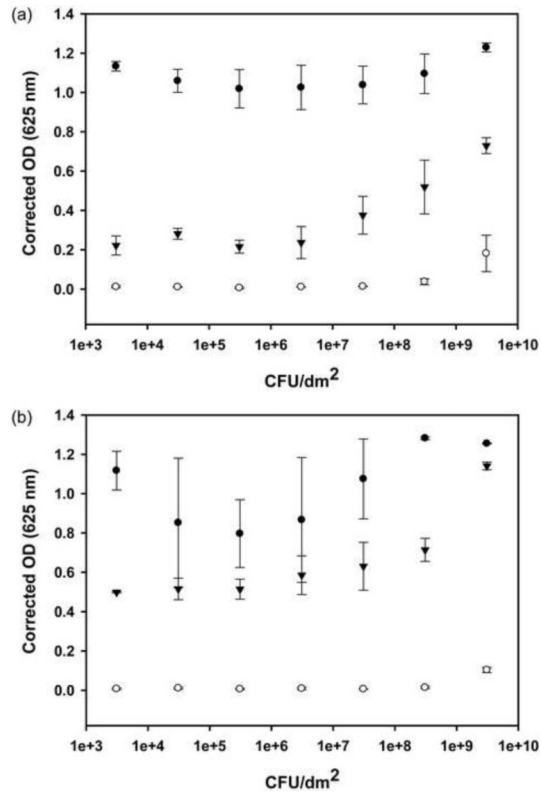
Fig. 6.
Polystyrene control surfaces (●), Gel-III (○) and PEGDA hydrogel (▲) surfaces challenged with an increasing number of CFUs of *E. coli* JM109 (a) or *S. aureus* ATCC25923 (b) for 48 h. (The bacterial density was calculated by dividing the initial bacterial CFUs by the bottom surface area of wells in the tissue culture plate)
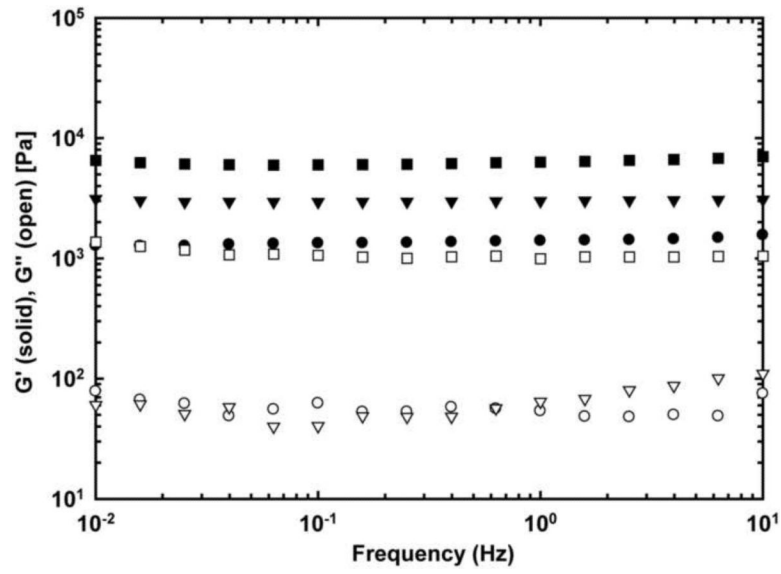
Fig. 7.
Storage modulus *G′* (solid symbols) and loss modulus *G″* (open symbols) as a function of frequency for Gel-III (●), Gel-VI (▲), and PEGDA gel (■).
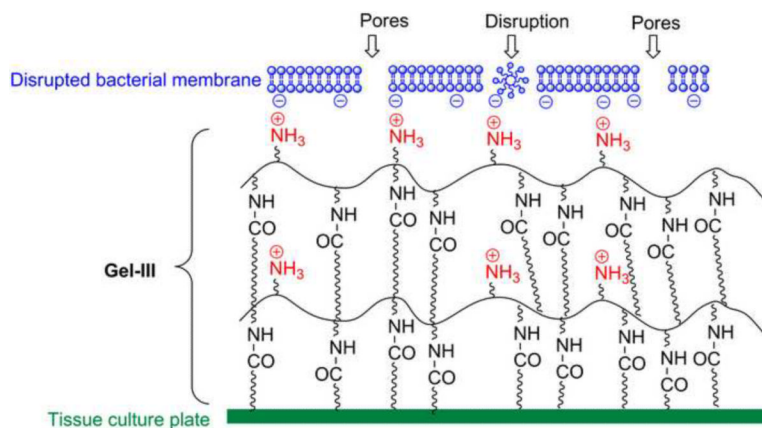
Fig. 8.
Schematic diagram of the interaction between the positively charged Gel-III and the negatively charged bacterial membranes. (Bacterial cytoplasmic membrane disruption may be caused by the rapid interaction of amphiphilic structure of AMP mimics and negatively charged lipid bilayers.)

Table 1

Polymerization Results.

Polypeptide	Expected M_n	$M_n{}^a$	$M_w{}^b$	PDI
Intermediate-1	22829	24459	44855	1.83
Intermediate-2	19685	19952	39184	1.96
Intermediate-3	16540	17265	33415	1.94
Intermediate-4	13396	14687	27584	1.88
Intermediate-5	10252	13714	25228	1.84

[a] Number-averaged molecular weight by GPC using a static light scattering and RI detection system.

[b] Weight-averaged molecular weight by GPC using a static light scattering and RI detection system.

Table 2

Hydrogel formation conditions.

Hydrogel	Polypeptide	Solubility of polypeptide in PBS buffer	Polypeptide stock solution		6-arm PEG-ASG stock solution		Final wt%		Final pH
			wt%	pH	wt%	pH	polypeptide	6-arm PEG-ASG	
Gel-I	Polypeptide-1	Very good	2.5	12	32	4	1.25	16	~ 7
Gel-II	Polypeptide-2	Very good	2.5	12	32	4	1.25	16	~ 7
Gel-III	Polypeptide-3	Very good	10	12	32	4	5	16	~ 7
Gel-IV	Polypeptide-4	Very good	10	12	32	4	5	16	~ 7
Gel-V	Polypeptide-5	Poor	10	12	32	4	5	16	~ 7
Gel-VI	trilysine	Very good	4	8	42	4	2	21	~ 7